Co-published by
**Institute of Fluid-Flow Machinery**
Polish Academy of Sciences
**Committee on Thermodynamics and Combustion**
Polish Academy of Sciences



http://www.imp.gda.pl/archives-of-thermodynamics/

# Darcy Forchheimer two-dimensional thin flow of Jeffrey nanofluid with heat generation/absorption and thermal radiation over a stretchable flat sheet

Saravanan Jagadha[a*], Batina Madhusudhan Rao[b], Putta Durgaprasad[c], Degavath Gopal[d], Putta Prakash[e], Naikoti Kishan[f], Krishnan Muthunagai[g]

[a]Institute of Aeronautical Engineering, Dundigal, Hyderabad, T.S. 500043, India
[b]Department of IT, Mathematics section, University of Technology and Applied Sciences, Muscat 324, Oman
[c]Vellore Institute of Technology, Kelambakkam - Vandalur Rd, Rajan Nagar, Chennai 600127, India
[d]Department of Mathematics, CMR Engineering College, Medchal, T.S. 501401, India
[e]Mohan Babu University, Sree Vidyanikethan Sree Sainath Nagar, Andhra Pradesh, Tirupati 517102, India
[f]Osmania University, Main road, Amberpet, Hyderabad, Telangana T.S. 500007, India
[g]Vellore Institute of Technology, Kelambakkam - Vandalur Rd, Rajan Nagar, Chennai, Tamil Nadu 600127, India

Received: 18.06.2023; revised: 23.12.2023; accepted: 19.04.2024

## Abstract

This work aims to study the combined effects of concentration and thermal radiation on a steady flow of Jeffrey nanofluid under the Darcy-Forchheimer relation over a flat nonlinear stretching sheet of variable thickness. A varying magnetic field influences normal to the flow movement is considered to strengthen the Jeffery nanofluid conductivity. However, a little effect of the magnetic Reynolds number is assumed to eliminate the impact of the magnetic field range. The higher-order nonlinear partial differential equations (PDEs) and convective boundary conditions are transformed into nonlinear ordinary differential equations (ODEs) by applying corresponding transformations. Then the ODEs are numerically solved with Runge-Kutta method via shooting technique. This process is applied for convergent relations of nanoparticle temperature, concentration, and velocity distributions. The influence of different fluid parameters like thermophoresis, melting parameter, Deborah number, chemical reaction parameter, Brownian motion parameter, inertia parameter and Darcy number on the flow profiles is explained through graphical analysis. Thermal radiation is emitted by accelerated charged particles, and the enhanced particle motion at higher temperatures causes a more significant discharge of radiation. Also, it was concluded that the heat generation parameter enhances the momentum boundary layer thickness and reduces the thermal and solutal boundary layer thickness over a Jeffrey nanofluid.

**Keywords:** MHD; Jeffrey nanofluid; Chemical reaction; Darcy-Forchheimer; Stretchable flat sheet

Vol. 45(2024), No. 2, 247–259; doi: 10.24425/ather.2024.150869

Cite this manuscript as: Jagadha, S., Madhusudhan Rao, B., Durgaprasad, P., Gopal, D., Prakash, P., Kishan, N., & Muthunagai, K. (2023). Darcy Forchheimer two-dimensional thin flow of Jeffrey nanofluid with heat generation/absorption and thermal radiation over a stretchable flat sheet. *Archives of Thermodynamics*, 45(2), 247-259.

## 1. Introduction

The analysis of boundary layer flow along with the radiation parameter is significant in different materials such as glass fabrications, liquid metallic fluids, and high-temperature plasmas. The specific transport problems seem to be highly nonlinear when combined with thermal convection fluid flows.

## Nomenclature

$a_0$, $b_0$ – constants
$B_0$ – stregth of magnetic field, kg/(s$^2$ A)
$C$ – fluid concentration
$C_{fx}$ – skin friction coefficient
$C_p$ – specific heat capacity at constant pressure, J/(kg K)
$C_\infty$ – fluid concentration in the free stream
$D_B$ – diffusion coefficient due to Brownian effect, m$^2$/s
$D_T$ – diffusion coefficient due to thermal effect, m$^2$/s
$D_\infty$ – diffusion of the fluid far away from sheet, m$^2$/s
Da – Darcy number
$F$ – dimensionless velocity
$k$ – porosity parameter
K – Deborah number
$k^*$ – absorption coefficient
Le – Lewis number
$M$ – magnetic field parameter
$n$ – shape parameter
$Nb$ – Brownian motion parameter
$Nt$ – thermophoresis parameter
$Nu_x$ – Nusselt number
$p$ – pressure, kg/(m s$^2$)
Pr – Prandtl number
$R$ – radiation parameter
Re – local Reynolds number
$Sh_x$ – Sherwood number
$T$ – temperature, K
$u$ – velocity component in $x$ direction, m/s
$v$ – velocity component in $y$ direction, m/s
$x$ – direction along the surface, m
$y$ – direction normal to the surface, m

### Greek symbols

$\alpha$ – thermal diffusivity, m$^2$/s
$\beta$ – interaction parameter
$\beta_s$ – heat generation parameter
$\varepsilon$ – variable thermal conductivity
$\Gamma$ – chemical reaction parameter
$\eta$ – similarity variable (dimensionless)
$\theta$ – dimensionless fluid temperature
$\lambda_s$ – concentration buoyancy parameter
$\lambda_t$ – thermal buoyancy parameter
$\upsilon$ – kinematic viscosity, m$^2$/s
$\xi$ – similarity variable
$\rho$ – fluid density, kg m$^{-3}$
$\sigma^*$ – Stefan-Boltzmann constant, W/(m$^2$ K$^4$)
$\tau$ – ratio of heat capacities
$\psi$ – stream function,
$\Phi$ – concentration in dimensionless form

### Subscripts and Superscripts

$\infty$ – ambient condition
$w$ – condition on surface
* – dimensionless properties
' – differentiation with respect to $\eta$

### Abbreviations and Acronyms

BL – boundary layer
CNT – carbon nanotubes
IVP – initial value problem
MBL – momentum boundary layer
MHD– magnetohydrodynamic
ODE – ordinary differential equation
PDE – partial differential equations

The distribution of temperature in the boundary layer is altered by the presence of thermal radiation at high temperatures, which affects the heat transfer near the wall. Because of their unique industrial applications, non-Newtonian liquid flows have attracted the interest of many researchers and scientists. Non-Newtonian fluids entitle a non-linear relation between stress and strain. The study of non-Newtonian flows and their features is not easy when compared to Newtonian fluids. To investigate the characteristics of non-Newtonian fluid flows, the Navier-Stokes equations are crucial. It has also been suggested to use a variety of fluid models to describe the properties of non-Newtonian liquids. One of the non-Newtonian liquids whose behaviour is being examined by means of a variety of models is Jeffrey fluid. Viscous fluids are developed using a single constitutive equation. There are several models of non-Newtonian materials accessible because these fluids have a variety of features that no single constitutive expression can adequately describe. The differential and rate-type liquid categories have gained the attention of numerous scholars. A significant non-Newtonian liquid that can determine the impact of retardation and relaxation is Jeffrey fluid. In bioengineering, geophysics, oil reservoir process, and chemical and nuclear technologies, Jeffrey fluid models are widely used. Many investigators, like Waqas [1] and Pal et al. [2] have studied and analysed Jeffrey fluid under various characteristics. Abdullah et al. [3] examined the magnetohydrodynamic (MHD) Jeffrey nanofluid flow over a stretching sheet. Turkyilmazoglu and Pop [4] discussed the flow and heat transfer of a Jeffrey fluid near the stagnation point on a stretching or shrinking sheet with a parallel external flow by using an analytical method. They observed the skin friction coefficient decreases as the stretching parameter of the sheet increases. Hayat et al. [5] reported on the MHD stagnation point flow of Jeffrey fluid near a stretching sheet with variable sheet thickness. They examined that the thermal boundary layer thickness increases with an increase in the heat generation parameter. Mabood et al. [6] studied the features of the heat flux model for a stagnation point flow of Jeffrey fluid past a flat stretching sheet. They observed that the momentum boundary thickness increases with an increase in Deborah number while decreasing the thermal boundary layer thickness.

Few researchers worked towards the combination of stretching sheet and thermal radiation influences on Jeffrey nanofluid. Using active energy and nonlinear thermal radiation effects, Hayat et al. [7] investigated the entropy generation optimisation of MHD Jeffrey nanofluid along a flat stretched surface. Technologies and businesses have investigated how to use the melting phenomenon. Researchers have focused on enhancing efficient, environmentally friendly, and energy-efficient systems.

These technologies are associated with planetary power and the recovery of excess heat. Three procedures (latent, sensible heat and chemical energy) have been implemented for energy storage. The MHD stagnation point flow of a Casson nanofluid as well as the combined effects of heat radiation and velocity slip were discussed by Besthapu et al. [8]. Kumar [9] later studied the differential transform method for transient hydro-magnetic Jeffrey liquid flow with a flat stretched sheet.

Many different fields, including heat exchanger coils, based pumps, solidification, and welding operations, etc., involve the melting phenomena. In addition to Newtonian cooling and nonlinear thermal radiation, Sen et al. [10] observed a thermal distributed homogeneous–heterogeneous interaction inside the MHD flow of Jeffrey fluid. By using the Fourier law and an infinite plate, Asjad et al. [11] modified the extended heat flux flow in Jeffrey fluid. Muhammad et al. [12] investigated a Jeffrey nanofluid flow under convective heat or mass circumstances. Anitha and Gireesha [13] explored the thermal analysis of Jeffrey nanofluid through microchannel applying Buongiorno's model. A stretched cylinder has been employed to examine the heat transfer analysis of Jeffrey nanofluid by Hayat et al. [14] and Ur Rasheed et al. [15]. Khan et al. [16] and Dadhich et al. [17] also examined the impact of thermal radiation on Jeffrey fluid. The different engineering and industrial applications such as heat transformers, chemical reactors and geothermic systems are associated with a convective permeable channel. The mechanical phenomenon, i.e. effect of diffusion and drag force, is dealt with in the Darcy-Forchheimer model. At first, it was known as the Darcian flow model, and as a modified Darcy-Forchheimer model was later extended toward nanofluid flow. This model was developed to explain the mechanical phenomenon in the analysis of heat flow in a fluid stream. The extra velocity term and drag force parameter in the equation of momentum, both of which have a negative sign, result in the Darcy-Forchheimer model. Several applications such as natural compound recovery strategy, soil material science, living tissue transitions, and junk storage (specifically gas litter) are included in this model. A few earlier investigations on the Darcy-Forchheimer model are reported by many researchers [18–20]. Seth and Mandal [21] employed the Darcy-Forchheimer model to analyse the Casson fluid flow. In connection with the Darcy-Forchheimer model, the problems concentrating on the fluid flows over a radially stretching sheet have attracted a huge number of researchers.

A notable amount of research was carried out on the problems of fluid flows due to nonlinear radially stretched surfaces. Bilal Ashraf et al. [22] studied MHD Jeffrey nanoliquid over a radially stretching surface along with radiative and mixed convection. Hayat et al. [23] examined the flow characteristics of Jeffrey fluid due to the nonlinear surface that can be stretchable in the radial direction. Ali et al. [24] incorporated a porous Reynolds number and a contracting/relaxing parameter in their analysis of the mass/heat transfer flow around metallic oxide nanoparticles close to perpendicularly moving extremely permeable discs. For the numerical results, they also used a correct quasi-linearization technique. Much research has introduced nonlinear stretching sheets into the Darcy-Forchheimer model of flow. Lund et al. [25] deliberated stability analysis of Casson nanoliquid flow past a stretchable exponential sheet with the help of the Darcy-Forchheimer model. Furthermore, the obtained results showed that several solutions occur only for high suction. In addition, the effect of a magnetic field is very useful in many chemical and engineering applications of nanoliquids. properties. In industries like thermal engineering, geothermal operations, chemical and petroleum equipment, etc., flow-saturating porous media is important.

Darcy law pays particular attention to permeable space. The Darcy principle is not intended for places where permeable channels experience increased flow rates because of uneven surrounding wall surfaces. Therefore, a non-Darcian effect resulting from a porous media is required to study the heat transfer and flow analysis. Khani et al. [27] examined the case of fluid flow saturating a non-Darcy permeable media with heat transfer. Hayat et al. [28] took into consideration the convective carbon nanotubes (CNTs) nanofluid flow over a non-Darcy permeable media. Siddiq et al. [29] and Madhu et al. [30] used the non-Darcy Forchheimer principle to evaluate the MHD radiative flow of the Carreau fluid to a stretching surface. They observed the Darcy-Forchheimer flow of MHD Powell-Eyring nanofluid past stretchable non-linear radial disc under the influence of activating energy. Later, problems with Darcy-Forchheimer MHD fluid flows were reviewed by Madkhali et al. [31], Machireddy et al. [32], Ramesh et al. [33] and Eswaramoorthi et al. [34]. Recently, the two-dimensional mixed convection and radiative Al2O3-Cu/H2O hybrid nanofluid flow over a vertical exponentially shrinking sheet with partial slip conditions has been analysed by Asghar et al. [35]. For this study, a physical model of the influence of thermal radiation on the two-dimensional flow of a hybrid nanofluid was developed. Asghar et al. [36] also investigated the effect of thermal radiation and the three-dimensional magnetized rotating flow of a hybrid.

The heat generation/absorption parameter is non-dimensional and depends on the amount of heat generated or absorbed in the fluid. The dual solutions of MHD Al2O3+Cu hybrid nanofluid in the presence of Joule heating were studied by Sajjad et al. [37]. Teh and Asghar [38] explained three-dimensional MHD hybrid nanofluid flow in the presence of Joule heating with a rotating stretching sheet. Furthermore, Asghar et al. [39–41] investigated the two-dimensional hybrid nanofluid flow with the effects of thermal slip condition, Joule heating and heat generation/heat absorption. Moreover, Gohar et al. [42] studied heat and mass transfer of Darcy-Forchheimer hybrid nanofluid flow due to an extending curved surface. Satyanarayana et al. [43] investigated nanofluid under the influence of suction/injection in a convective medium. Mamatha et al. [44] discussed the mass transfer analysis of two-phase flow in a suspension of microorganisms. Finally, Madhusudhana Rao et al. [45] studied the heat and mass transfer mechanism on the three-dimensional flow of inclined magneto Carreau nanofluid with chemical reaction.

The goal of the current study, which was motivated by the research, is to identify a Darcy Forchheimer 2D thin flow of Jeffrey nanofluid with heat generation or absorption and thermal radiation over a stretchable flat sheet. Under the relevant boundary conditions, the coupled nonlinear PDEs can be numerically solved using the MATLAB solver with the help of the Runge-Kutta method via shooting technique. The effects of physical parameters on the fluid concentration ($\Phi(\xi)$) and temperature ($\theta(\xi)$), and the velocity field ($F'(\xi)$), are graphically displayed for numerous sets of physical parameter values. The thermophoresis parameter enhances the heat transfer rate and decelerates the mass transfer rate. Also, it was observed that the thermal radiation parameter increases the heat transfer rate.

## 2. Mathematical analysis

Let us consider a steady a two-dimensional laminar and incompressible magnetohydrodynamic flow of Jeffrey nanofluid with heat generation or absorption and thermal radiation over a stretchable flat sheet, as shown in Fig. 1.

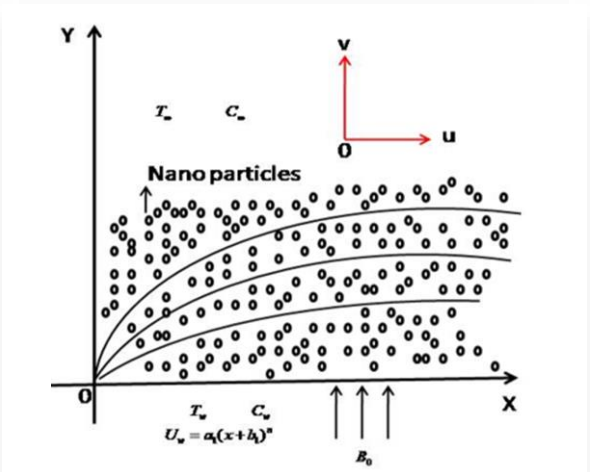


Fig. 1. Physical description of the problem.

After employing the usual boundary layer analysis, the basic partial differential equations governing the conservation of mass, momentum, energy, and concentration for the Jeffrey nanofluid flow can be written as, respectively [46].

$$u_x + v_y = 0, \tag{1}$$

$$u\,u_x + v\,u_y = \frac{\upsilon}{(1+\lambda_s)}\left[\upsilon\,u_{yy} + \lambda_t\left(v\,y_{yyy} + u\,u_{xyy} + u_y u_{xy}\right) - \left(\frac{\sigma^2 B_0^2}{\rho} + \frac{\upsilon\varepsilon}{k}\right)u - \frac{\varepsilon c_b}{\sqrt{k}}u^2 u_x u_{xy}\right], \tag{2}$$

$$\left(u\,T_x + v\,T_y\right) = \alpha T_{yy} + \tau\left(D_B C_y T_y + \frac{D_T}{T_\infty}T_y^2\right) + \frac{16\sigma^* T_\infty^3}{3k^*\rho c_p}T_{yy} + \frac{Q_0(T_0 - T_m)}{\rho c_p}, \tag{3}$$

$$\left(u\,C_x + v\,C_y\right) = D_B C_{yy} + \frac{D_T}{T_\infty}T_{yy} - K_n(C - C_w)^m, \tag{4}$$

where $u$ and $v$ represent the velocity vector components in $x$ and $y$ directions, respectively, $\upsilon$ is the kinematic viscosity, $\rho$ is the fluid density, $c_p$ is its specific heat, $\varepsilon$ is the variable thermal conductivity, $k$ is the permeability, $B_0$ is the strength of the magnetic field, $c_b$ is the drag force, whereas $\lambda_s$ and $\lambda_t$ denote the concentration and thermal buoyancy parameters, respectively. Parameters $D_B$ and $D_T$ represent Brownian and thermal diffusivities, respectively, $T$ is the field temperature, $\alpha$ denotes thermal diffusivity, $C$ is the fluid concentration, $Q_0$ is the heat generation/absorption, $\tau$ is the ratio of heat capacities., $\sigma^*$ and $k^*$ represent the Stefan-Boltzmann constant and the absorption coefficient, respectively, and $K_n$ stands for the $n$-th order chemical reaction. Subscripts $\infty$ and $w$ refer to free stream (ambient) and surface (wall), respectively.

Boundary conditions near and away from the sheets surface were described as:

$$\begin{cases} u = u_w(x) = a_0(x + b_0)^n, v = 0, T = T_w, C = C_w & \text{at } y = \delta(x + b_0)^{\frac{(1-n)}{2}} \\ T \to T_\infty, C \to C_w, u \to 0 & \text{as } y \to \infty \end{cases}. \tag{5}$$

Introducing the non-dimensional quantities:

$$\psi(x, y) = \sqrt{\frac{2\upsilon a_0}{n+1}(x + b_0)^{n+1}}\, f(\eta), \tag{6a}$$

$$\eta = y\sqrt{\frac{(n+1)}{2\upsilon}(x + b_0)^{n-1}}, \tag{6b}$$

$$u = a_0(x + b_0)^n f'(\eta), \tag{6c}$$

$$v = -\sqrt{\frac{\upsilon(n+1)}{2}a_0(x + b_0)^{n-1}}\left(f(\eta) + \eta\left(\frac{n-1}{n+1}\right)\right)(x + b_0)^n f'(\eta), \tag{6d}$$

$$\theta(\eta) = \frac{T - T_w}{T - T_\infty},\ \ \Phi(\eta) = \frac{C - C_w}{C - C_\infty}, \tag{6e}$$

the set of dimensionless form of the governing Eqs. (2)–(4) along with the boundary conditions (Eq. (5)) are converted to the set of ODEs as:

$$F''' - \mathrm{K}\left[\left(\frac{n-1}{2}\right)F'F^{iv} - (n-1)F'F''' - \left(\frac{3n-1}{2}\right)F''^2\right] - \left(\frac{2n}{n+1}\right)(1+\lambda_s)F'^2 - \left(\frac{2}{n+1}\right)(1+\lambda_s)\left(MF' - \beta F'^2 - \mathrm{Da}F'\right) = 0, \quad (7)$$

$$\frac{1}{\mathrm{Pr}}\left(1+\frac{4R}{3}\right)\theta'' + f\theta' + Nt\theta'\Phi' + \frac{2}{n+1}\lambda\theta = 0, \quad (8)$$

$$\Phi'' + \mathrm{PrLe}\Phi' + \frac{Nt}{Nb}\theta'' + \Gamma\Phi^m = 0, \quad (9)$$

where K, Da, Pr, and Le are the Deborah, Darcy, Prandtl and Lewis numbers, respectively, *R* is a thermal radiation parameter, *M* is a magnetic field parameter, *Γ* denotes a chemical reaction parameter, *n* is a shape factor, whereas *Nt* and *Nb* are the thermophoresis and Brownian motion parameters. Parameter *β* represents inertia parameter.

The corresponding non-dimensional boundary conditions are:

$$\begin{cases} \Phi(0) = 0, F'(0) = 1, \theta(0) = 0, F(0) = 0 \\ F'(\infty) \to 0,\ \theta(\infty) \to 0, \Phi(\infty) \to 0 \end{cases}, \quad (10)$$

where the parameters in the Eqs. (7)–(9) are assumed as:

$$M = \sqrt{\frac{\sigma}{a\rho}}B_0, \mathrm{Pr} = \frac{\upsilon}{\alpha}, \mathrm{Le} = \frac{\alpha}{D_B}, \mathrm{Da} = \frac{\upsilon\varepsilon}{ka_0(x+b_0)^{n-1}},$$

$$Nt = \frac{\tau D_T(T_w - T_\infty)}{\upsilon T_\infty}, Nb = \frac{\tau D_B(C_w - C_\infty)}{\upsilon}, R = \frac{4\sigma^* T_\infty^3}{kk^*},$$

$$\beta = \frac{\varepsilon C_b(x+b_0)}{\sqrt{k}}, \Gamma = xK_n(C_w - C_\infty)^{n-1}.$$

For engineering interest, skin friction coefficient, Nusselt and Sherwood numbers are represented as, respectively:

$$C_{fx} = \frac{\tau}{\frac{1}{2}\rho u_w^2}, \mathrm{Nu}_x = \frac{(x+b_0)q_w}{k(T_w - T_\infty)}, \mathrm{Sh}_x = \frac{(x+b_0)q_m}{D_B(C_w - C_\infty)},$$

where $q_w$ is the heat flux and $q_m$ represents the mass flux.

With the help of non-dimensional variables (Eqs. (6)), the aforementioned $C_{fx}$, $\mathrm{Nu}_x$ and $\mathrm{Sh}_x$ are rewritten as:

$$\mathrm{Re}^{\frac{1}{2}} C_{fx} = \frac{1}{1+\lambda_s}\left(F''(0) + K\left(F'(0)\right)F''(0) + -\left(\frac{n+1}{2}\right)F(0)F'''(0)\right),$$

$$\mathrm{Re}^{-\frac{1}{2}}\mathrm{Nu}_x = -(1+R)\sqrt{\frac{n+1}{2}}\,\theta'(0);$$

$$\mathrm{Re}^{-\frac{1}{2}}\mathrm{Sh}_x = -\sqrt{\frac{n+1}{2}}\,\Phi'(0),$$

or

$$\mathrm{Re}^{-\frac{1}{2}}\mathrm{Sh}_x = -\frac{a_0(x+b_0)^{n+1}}{\upsilon}$$

where $\mathrm{Sh}_x$ is the local Sherwood number due to stretching velocity.

## 3. Solution methodology

The familiar numerical technique Runge-Kutta method of fourth order was employed to obtain solutions of non-linear governing flow ordinary differential equations (7)–(9) subjected to boundary conditions (10). The nonlinear derivative formations are reduced to simultaneous mathematical formulations. The initial input value of the similarity variable is taken as zero and the free streamline as infinity for ($F'$,$\theta$,$\Phi$). An infinity condition was presented for the free streamline but in the calculation, the maximum value of η is taken as 7. This value is appropriate to satisfy the flow region conditions for all the physical significances of dimensionless parameters.

Higher-order differential equations are converted to linear formulations by introducing new variables:

$$(f_1 = F), (f_2 = F'), (f_3 = F''), (f_4 = F'''), (f_5 = \theta),$$

$$(f_6 = \theta'), (f_7 = \Phi), (f_8 = \Phi').$$

Equations (7)–(9) are transformed into the following first-order ODEs:

$$f_4' = \frac{1}{k\left(\frac{n+1}{2}\right)f_2}\left[f_4 - k\left(-(n-1)f_2f_4 - \left(\frac{3n-1}{2}\right)f_3^2\right)\left(\frac{2n}{n+1}\right)(1+\lambda_s)f_2^2 - \left(\frac{2}{n+1}\right)(1+\lambda_s)[Mf_2 - \beta f_2^2 - \mathrm{Da}f_2]\right], \quad (11)$$

$$f_6' = \frac{1}{Pr\left(1+\frac{4R}{3}\right)}\left[f_1f_6 + Ntf_6^2 + Nbf_6f_8 + \left(\frac{2}{n+1}\right)\lambda f_5\right], \quad (12)$$

$$f_8' = -\left[\mathrm{Pr}\,Le\,f_1f_8 + \frac{Nt}{Nb}f_6 + \Gamma f_7^m\right]. \quad (13)$$

The results of governing flow equations of Jeffrey nanofluid were approximated numerically using MATLAB bvp4c software [47] for the interpretation of dimensionless quantifiers.

## 4. Algorithm

The solution algorithm includes the following steps:

- First, the momentum, energy and conservation equations are converted into IVP (initial value problem) equations, as stated in Eqs. (11)–(13).
- The solvers continually call the ordinary differential equation (ODE) file to assess the system of differential equations at different times (for energy equations and momentum). These are the data (information) required to be defined for the ODE system to be computed.
- The switch statement governs the type of output required so that the ODE file can pass the appropriate information (data) to the solver. In the default initial conditions ('bvpinit') case, the ODE file returns basic information (time span, initial conditions, and options) to the solver.
- In the 'Jacobian' case, the MATLAB ODE45 file returns a Jacobian matrix to the solver. If the Jacobian value becomes an undefined value (infinity) an error is received, so there is a need to change the guess values and proceed further.
- The physical governing parameters are guessed based on existing information like magnetic field, thermal radiation, thermal buoyancy, etc.

Once all the initial conditions are found, the solver automatically gives the plots as well as values in the command window.

## 5. Results and discussion

In this work, the combined effects of heat generation/absorption, melting heat transfer, and thermal radiation were investigated for the 2-D Darcy Forchheimer flow of a Jeffrey nanofluid past a flat stretchable sheet. Using the Runge-Kutta and shooting technique, the basic Eqs. (7)–(9) and boundary conditions Eq. (10) were solved. For evaluating the consistency and accuracy of the solutions, numerical analysis of influence of the significant parameters are demonstrated through graphs in this section. To obtain the results, numerical computations are carried out by assuming different values of non-dimensional governing parameters such as: $R = 1.1$, $M = 0.2$, $Nt = 0.2$, $Nb = 0.1$, Da = 0.5, $\beta = 1$, $\beta_s = 0.6$, $n = 0.3$, and Pr = 0.3.

The significance of radiation parameter ($R$) on the temperature profile $\theta(\xi)$ is interpreted through Fig. 2. It may be observed that an increase in thermal radiation parameter raises the fluid temperature over a flat stretching sheet since thermal radiation powers the varying temperatures to exchange energy. The particles move more rapidly due to higher kinetic energy. More particle collisions and more significant acceleration of charged particles result from this increased heat radiation. Accelerated charged particles are the source of electromagnetic radiation or thermal radiation, and the enhanced particle motion at higher temperatures causes a more significant discharge of radiation.

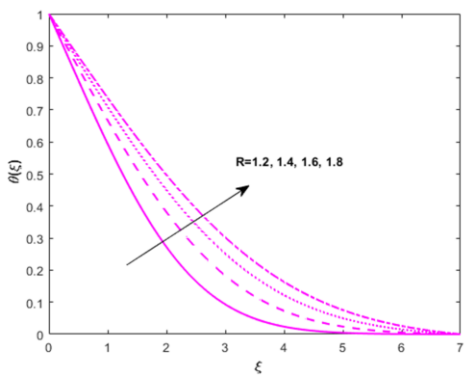


Fig. 2. Impact of $R$ on $\theta(\xi)$.

Figures 3a and 3b show the effect of shape parameter $n$ on the distributions of nanofluid concentration and temperature, respectively, in presence of stretching sheet. It is perceived that both concentration and temperature decrease for the incremental values of shape parameter.

From Figs. 4(a) and 4(b), illustrating the impact of thermophoresis quantity ($Nt$) on $\Phi(\xi)$ and $\theta(\xi)$, it is found that both profiles enlarge for improved values of $Nt$ in the case of heat generation. Hence, it can be inferred that the amount of heat and mass exchange will be increased by enhancing $Nt$. In fact, solid nanoparticles in the nanofluid experience a force in the direction opposite to the imposed temperature gradient. Hence, the nanoparticles tend to move from hot to cold. It is important to note that the thermophoresis parameter is positive when the temperature of the wall is higher than the ambient temperature.

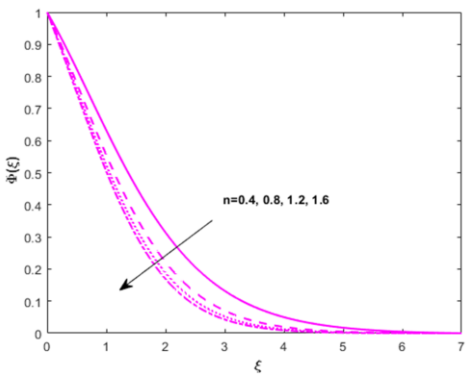


(a)

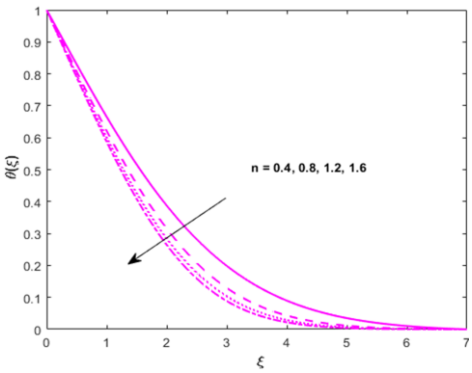


(b)

Fig. 3. Impact of $n$ on: a) $\Phi(\xi)$, b) $\theta(\xi)$.

Through Figs. 5a, 5b and 5c, the effect of the magnetic field parameter ($M$) on the velocity field ($F'(\xi)$), temperature $\theta(\xi)$ and concentration ($\Phi(\xi)$), respectively, is illustrated and explained.

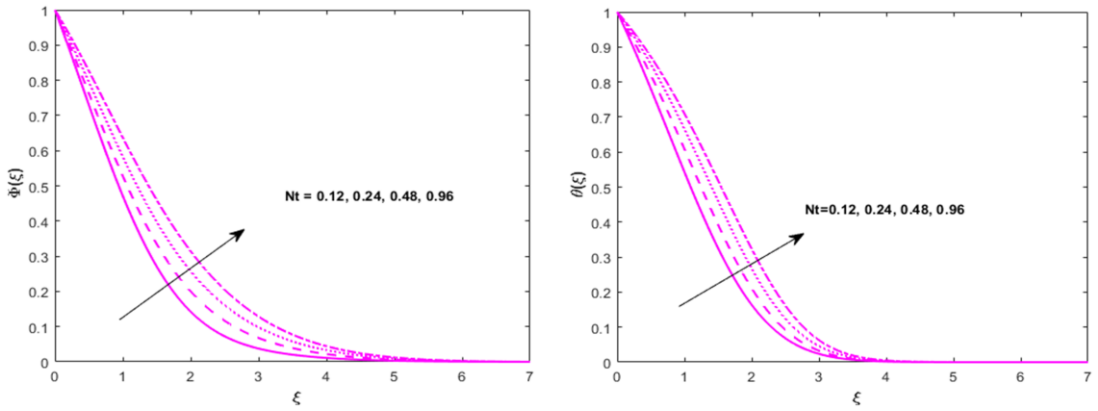


(a) (b)

Fig. 4. Effect of *Nt* on: a) $\Phi(\zeta)$, b) $\theta(\zeta)$.

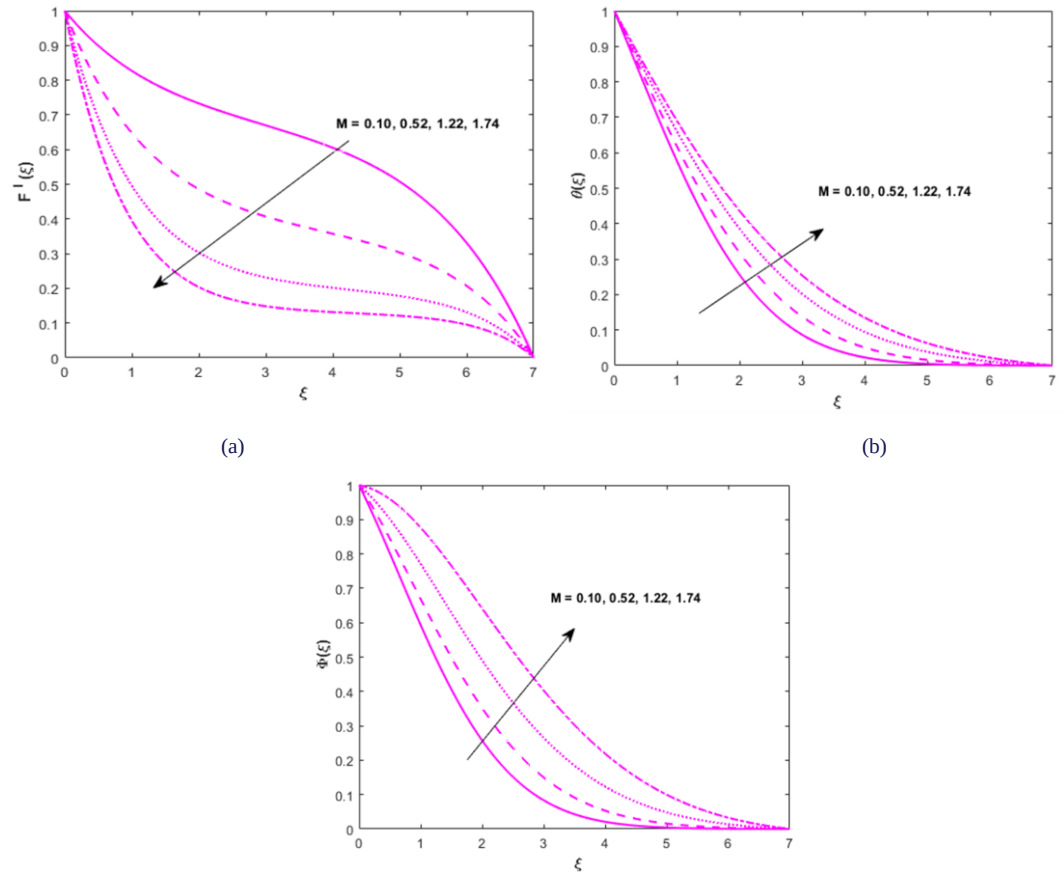


(a) (b)

(c)

Fig. 5. Influence of *M* on: a) $F'(\zeta)$, b) $\theta(\zeta)$, and c) $\Phi(\zeta)$.

These results show that the magnetic field reduces the fluid velocity by lowering the resistive force, known as the Lorentz force, whereas $\theta(\zeta)$ and $\Phi(\zeta)$ rise for improved values of *M* in the presence of stretching sheet. It is also found that the increased magnetic parameter results in the concentration increase for both stretching and shrinking sheets.

The influence of Deborah number (K) on temperature and concentration profiles of Jeffrey nanofluid is presented in Figs. 6a and 6b, respectively. The increasing Deborah number enhances the temperature rise over the stretching sheet since the extrapolated temperature depends on the mechanical properties of polymers. The Deborah number increases the concentration of nanofluid, which causes a reduction in the momentum boundary layer (MBL) and a rise in the thermal boundary layer (TBL).

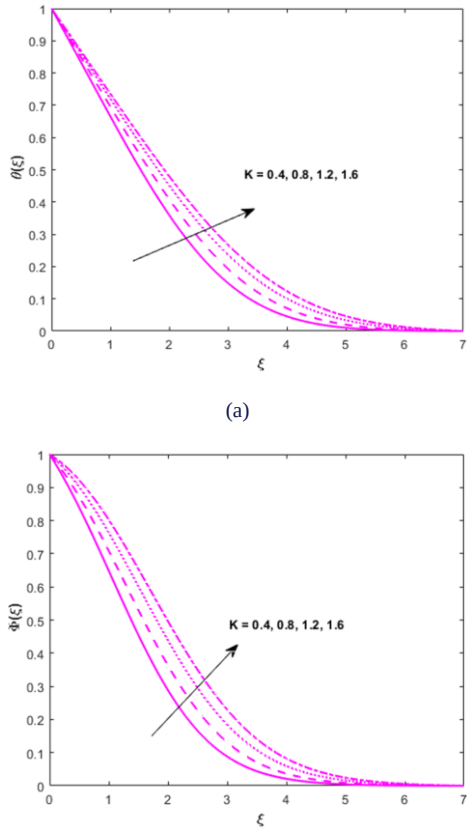


Fig. 6. Influence of K on: a) $\theta(\zeta)$, and b) $\Phi(\zeta)$.

The impact of Darcy number (Da) on flow velocity, temperature, and concentration of nanofluid past stretchable flat sheet is illustrated through Figs. 7a, 7b and 7c, respectively. It can be noticed noticed that the Darcy number accelerates the nanofluid flow and declines the temperature and concentration profiles of the nanofluid. Hence, it is concluded that an increasing Darcy number speeds up the motion of fluid particles, but it reduces the temperature of fluid near the stretching sheet.

The concentration of nanofluid flow via a flat stretching sheet is depicted in Fig. 8 exhibiting the effect of a chemical reaction parameter ($\Gamma$), which increases the concentration of nanofluid close to the wall. The concentration of nanoparticles close to the surface may be dominated by chemical processes if the chemical reaction parameter has a greater value. A lower value denotes a greater influence of other variables, such as convective transport.

It is observed from Figs. 9a and 9b that growing $\beta$ raises up $\theta(\zeta)$ and $\Phi(\zeta)$ of a nanofluid over the stretching surface.

The influence of heat generation parameter $\beta_s$ on $F'(\zeta)$, $\theta(\zeta)$ and $\Phi(\zeta)$ of the nanofluid past the stretchable non-linear flat sheet is displayed in Figs. 10a, 10b and 10c, respectively. It can be noticed that nanofluid velocity enlarges as the heat generation parameter increases. The impact of $\beta_s$ results in reducing the temperature of the fluid. In addition, the direction of heat transfer is turned around all through heat generation.

The impact of heat generation or absorption through a stretched surface on the concentration of nanofluid and the

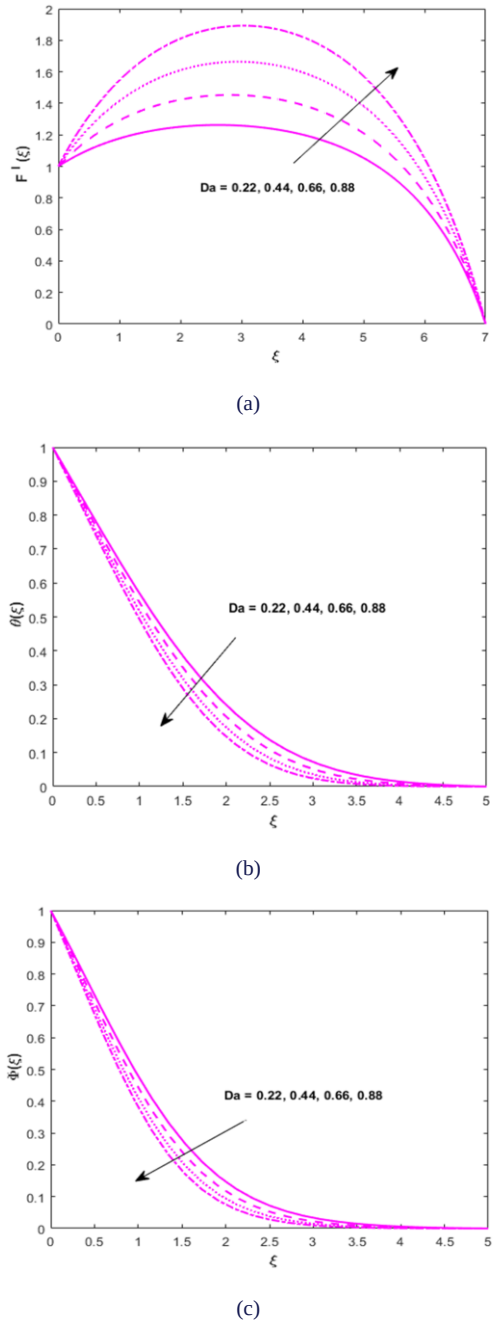


Fig. 7. Influence of $M$ on: a) $F'(\zeta)$, b) $\theta(\zeta)$, and c) $\Phi(\zeta)$.

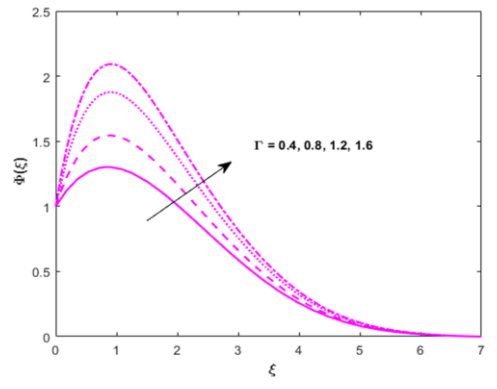


Fig. 8. Effect of $\Gamma$ on $\Phi(\zeta)$.

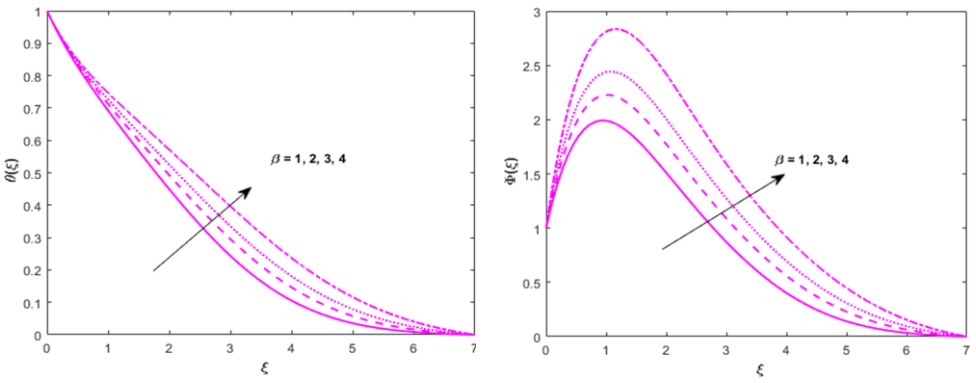


(a) (b)

Fig. 9. Impact $\beta$ on: a) $\theta(\zeta)$, and b) $\Phi(\zeta)$.

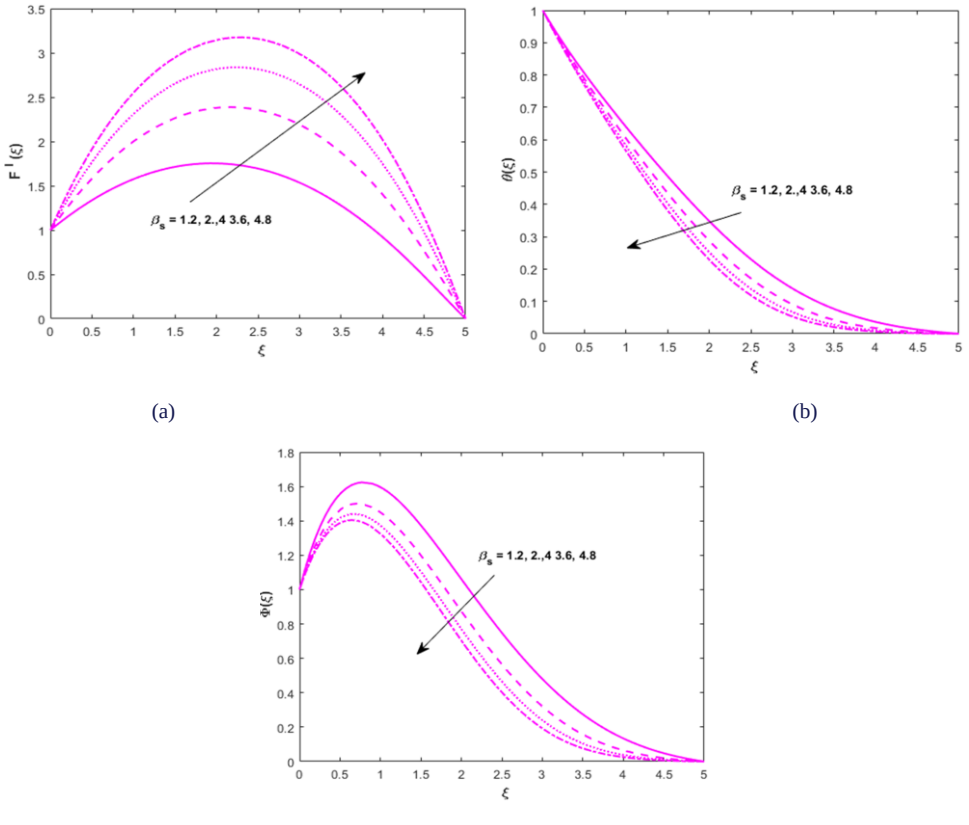


(a) (b)

(c)

Fig. 10. Effect of $\beta_s$ on: a) $F'(\zeta)$, b) $\theta(\zeta)$, and c) $\Phi(\zeta)$.

thickness of the thermal boundary layer is also examined. The impact of Brownian motion parameter ($Nb$) on $\theta(\zeta)$ and $\Phi(\zeta)$ is exhibited through the Figs. 11a and 11b, respectively. The results show that the augmented Brownian movement enhances the temperature profile whereas it decrements the concentration of Jeffrey nanofluid past the stretching sheet.

Figure 12 demonstrates the influence of Prandtl number (Pr) on $\Phi(\zeta)$ and $\theta(\zeta)$. The results show that an increase in Pr decreases the concentration $\Phi(\zeta)$ and it surges up the $\theta(\zeta)$ of the nanofluid along the stretching sheet.

Figure 13 displays the impact of the Lewis number (Le) on the concentration of nanofluid flow. A dimensionless number known as the Lewis number is defined as the ratio of the thermal boundary thickness to the concentration boundary layer thickness. The results reveal that the Lewis number reduces the concentration of nanofluid past the stretching surface. When it increases, the fraction of nanoparticle volume increases and the rate of mass transfer increases.

From Table 1 we can observe that $M$, $\beta$ and $Nt$ decrease the skin friction factor coefficient, and heat and mass transfer rates,

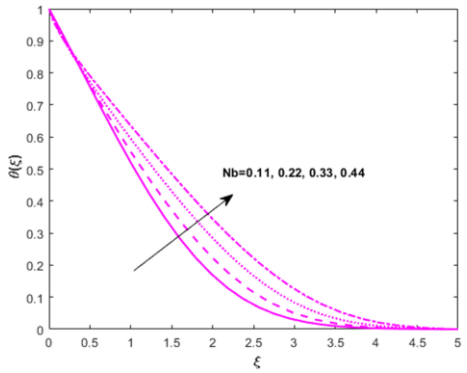


(a)

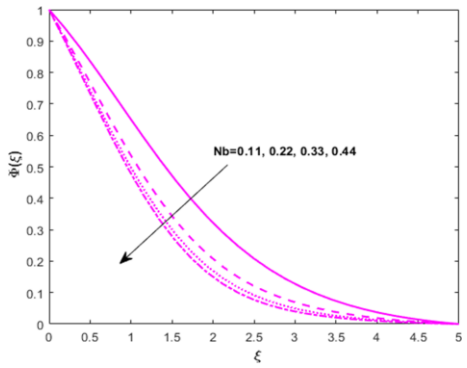


(b)

Fig. 11. Impact of *Nb* on: a) $\theta(\zeta)$, and b) $\Phi(\zeta)$.

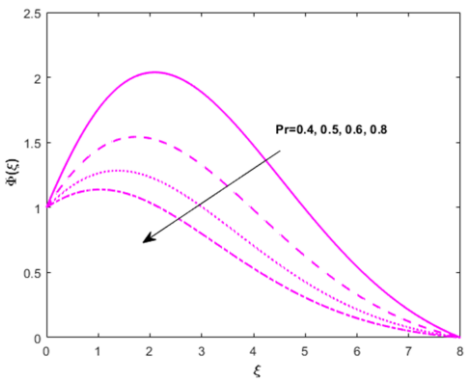


(a)

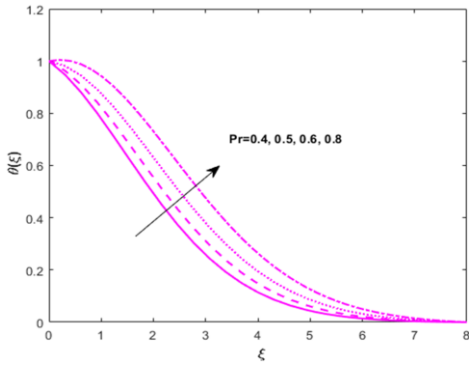


(b)

Fig. 12. Effect of Pr on: a) $\Phi(\zeta)$, and b) $\theta(\zeta)$.

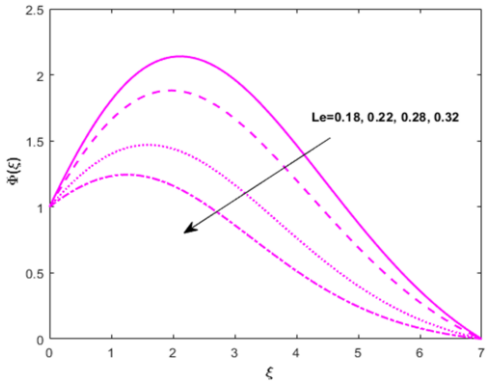


Fig. 13. Effect of Le on $\Phi(\zeta)$.

but the opposite trend can be observed as regards the impact of chemical reaction parameter. Darcy parameter and heat source parameter enhance the heat and mass transfer rates but diminish the skin friction coefficient. Finally, the Prandtl number and thermal radiation parameter enhance the heat transfer rate. The goal of this work is to show that the thermophoresis parameter impacts flat stretching sheet irrespective of additional physical characteristics. A comparison of previous findings was used to evaluate the validity of the present analysis. Heat generation, chemical reaction, thermal relaxation, thermal radiation, Lewis number, Prandtl number, and Brownian motion parameters are found to be in excellent agreement with those of Noghrehabadi et al. [48] and Rasool et al. [49], which are shown in Table 2.

## 6. Concluding remarks

The present work investigates the influence of the rate of heat and mass transfer on the boundary layer flow of a Jeffrey fluid. Some of the key findings of the study are listed below:

1) An increase in the thermal radiation parameter ($R$) leads to an increase in $\theta(\zeta)$ over the flat stretching sheet and the shape parameter ($n$) decreases both concentration and temperature profiles.
2) The concentration ($\Phi(\zeta)$) enlarges for improved metrics of thermophoresis parameter ($Nt$) in heat generation and hence, it could be inferred that the amount of heat and mass exchange increases by enhancing the thermophoresis parameter.
3) The magnetic field parameter ($M$) lessens the fluid velocity $F'(\zeta)$, whereas it increases both temperature and concentration in the presence of stretching sheet.
4) The fluid velocity increases, and both, temperature and concentration, decrease over the stretching sheet for increasing values of Deborah number (Da).
5) Da accelerates the flow and the interaction parameter ($\beta$) declines temperature and concentration profiles. The concentration of nanofluid near the wall enlarges as chemical reaction parameter ($\Gamma$) increases.
6) An increase in $\beta$ augments the temperature and concentration of the nanofluid over stretching sheet.

Table 1. Numerical values of $\mathrm{Re}^{1/2}C_{fx}$, $-\mathrm{Re}^{-1/2}\mathrm{Nu}_x$ and $-\mathrm{Re}^{-1/2}\mathrm{Sh}_x$ for distinct values of $n$, $M$, $\lambda$, Le, $Nb$, $Nt$.

| $M$ | $R$ | $n$ | $\beta$ | $Nb$ | $Nt$ | Pr | Da | $\beta_s$ | $\Gamma$ | $\mathrm{Re}^{1/2}C_{fx}$ | $-\mathrm{Re}^{-1/2}\mathrm{Nu}_x$ | $-\mathrm{Re}^{-1/2}\mathrm{Sh}_x$ |
|---|---|---|---|---|---|---|---|---|---|---|---|---|
| 0.2 | 1.1 | 0.3 | 1.0 | 0.2 | 0.1 | 0.3 | 0.5 | 0.6 | 0.3 | -0.282825 | 0.470756 | 0.296402 |
| 0.4 | | | | | | | | | | -0.405691 | 0.447773 | 0.257508 |
| 0.8 | | | | | | | | | | -0.613039 | 0.407362 | 0.175855 |
| | 1.1 | | | | | | | | | -0.462033 | 0.508971 | 0.260833 |
| | 2.2 | | | | | | | | | -0.462132 | 0.627797 | 0.285551 |
| | 3.3 | | | | | | | | | -0.462153 | 0.743016 | 0.299653 |
| | | 0.3 | | | | | | | | -0.455331 | 0.834993 | 0.430956 |
| | | 0.6 | | | | | | | | -0.232639 | 1.404371 | 0.623115 |
| | | 0.9 | | | | | | | | -0.120835 | 1.983364 | 0.776368 |
| | | | 1.0 | | | | | | | -0.911888 | 0.350850 | 0.144496 |
| | | | 1.5 | | | | | | | -1.032867 | 0.340127 | 0.084824 |
| | | | 2.0 | | | | | | | -1.141087 | 0.331808 | 0.022914 |
| | | | | 0.2 | | | | | | -0.613312 | 0.373469 | 0.100882 |
| | | | | 0.4 | | | | | | -0.725521 | 0.360514 | 0.022858 |
| | | | | 0.8 | | | | | | -0.816602 | 0.339530 | 0.084342 |
| | | | | | 0.1 | | | | | -0.816602 | 0.353799 | 0.100335 |
| | | | | | 0.3 | | | | | -0.816602 | 0.346146 | 0.208557 |
| | | | | | 0.6 | | | | | -0.816602 | 0.339346 | 0.701374 |
| | | | | | | 0.3 | | | | -0.865965 | 0.293768 | 0.789873 |
| | | | | | | 0.5 | | | | -0.865975 | 0.399425 | 0.369492 |
| | | | | | | 0.7 | | | | -0.865985 | 0.468570 | 0.196080 |
| | | | | | | | 0.5 | | | -0.692204 | 0.415457 | 0.301114 |
| | | | | | | | 0.7 | | | -0.578540 | 0.436285 | 0.339561 |
| | | | | | | | 0.9 | | | -0.451867 | 0.459372 | 0.381474 |
| | | | | | | | | 0.6 | | -0.503356 | 0.502596 | 0.154077 |
| | | | | | | | | 1.2 | | -0.503353 | 0.461514 | 0.156926 |
| | | | | | | | | 1.8 | | -0.503350 | 0.454051 | 0.226907 |
| | | | | | | | | | 0.4 | -0.503356 | 0.465296 | 0.159757 |
| | | | | | | | | | 0.8 | -0.503355 | 0.527696 | 0.553727 |
| | | | | | | | | | 1.2 | -0.428455 | 0.876910 | 0.929316 |

Table 2. Comparison of the present study results with other research findings, for $-\Phi'(0)$ and various values of $Nt$, with $R = M = Nt = \mathrm{Da} = \beta = \beta_s = \Gamma = 0$, $Nb = 0.2$, Pr = 10 and Le = 10.

| $Nt$ | $-\Phi'(0)$ | | |
|---|---|---|---|
| | Noghrehabadi et al. [48] | Rasool et al. [49] | Present results |
| **0.2** | 1.76895455 | 1.76895455 | 1.76862 |
| **0.4** | 2.09565585 | 2.09565585 | 2.09544 |
| **0.6** | 2.50535461 | 2.50535461 | 2.50522 |

7) The velocity enlarges as heat generation parameter increases and the impact of heat absorption/generation outcomes in reducing $\theta(\zeta)$ and $\Phi(\zeta)$ distributions of the fluid over stretching sheet.
8) Chemical reaction parameter enhances the mass transfer rate in a Jeffrey nanofluid.
9) Thermophoresis and Brownian motion parameters decrease the heat transfer.

## References


[1] Waqas, H. (2021). Numerical simulation for magnetic dipole in bio convection flow of Jeffrey nanofluid with swimming motile microorganisms. *Waves in Random and Complex Media*, 1–18. doi: 10.1080/17455030.2021.1948634

[2] Pal, D., Mondal, S., & Mondal, H. (2019). Entropy generation on MHD Jeffrey nanofluid over a stretching sheet with nonlinear thermal radiation using spectral quasilinearization Method. *International Journal of Ambient Energy*, 42(15), 1712–1726. doi: 10.1080/01430750.2019.1614984

[3] Abdullah Mohamed, R.A. (2020). MHD Jeffrey nanofluid flow over a stretching sheet through a porous medium in presence of nonlinear thermal radiation and heat generation/absorption. *Transport Phenomena in Nano and Micro Scales*, *8*(1), 9–22. doi: 10.22111/TPNMS.2019.29314.1172

[4] Turkyilmazoglu, M., & Pop, I. (2013). Exact analytical solutions for the flow and heat transfer near the stagnation point on a stretching/shrinking sheet in a Jeffrey fluid. *International Journal of Heat and Mass Transfer*, 57, 82–88. doi: 10.1016/ j.ijheatmasstransfer.2012.10.006

[5] Hayat, T. (2018). Simultaneous effects of melting heat and internal heat generation in stagnation point flow of Jeffrey fluid towards a nonlinear stretching surface with variable thickness. *International Journal of Thermal Sciences*, 132, 344–354. doi: 10.1016/j.ijthermalsci.2018.05.047

[6] Mabood, F., Imtiaz, M., & Hayat, T. (2020). Features of Cattaneo-Christov heat flux model for Stagnation point flow of a Jeffrey fluid impinging over a stretching sheet: A numerical study. *Heat Transfer*, 49(5), 2706–2716. doi: 10.1002/htj.21741

[7] Hayat, T., Kanwal, M., Qayyum, S., & Al Saedi, A. (2020). Entropy generation optimization of MHD Jeffrey nanofluid past a stretchable sheet with activation energy and non-linear thermal radiation. *Physica A*, 544, 123457. doi: 10.1016/j.physa.2019.123437

[8] Besthapu, P., Ul Haq, R., Bandari, S., & Al-Mdallal, Q.M. (2019). Thermal radiation and slip effects on stagnation point flow of

MHD non-Newtonian nanofluid over a convective stretching surface. *Neural Computing and Applications*, 31, 207–221. doi: 10.1007/s00521-017-2992-x

[9] Kumar, M. (2020). Study of differential transform technique for transient hydromagnetic Jeffrey fluid flow from a stretching sheet. *Nonlinear Engineering*, 9, 145–155. doi: 10.1515/nleng-2020-0004

[10] Sen, S.S.S., Das, M., & Shaw, S. (2021). Thermal dispersed homogeneous- heterogeneous reaction within MHD flow of a Jeffrey fluid in the presence of Newtonian cooling and nonlinear thermal radiation. *Heat Transfer*, 50(6), 5744–5759. doi: 10.1002/htj.22146

[11] Asjad, M.I., Basit, A., Akgul, A., & Muhammad, T. (2021). Generalized thermal flux flow for Jeffrey fluid with Fourier law over an infinite plate. *Mathematical Problems in Engineering*, 5403879. doi: 10.1155/2021/5403879

[12] Muhammad, K., Hayat, T., & Alsaedi, A. (2021). Stagnation point flow of Jeffrey nanofluid with activation energy and convective heat and mass conditions. In *Proceedings of the Institution of Mechanical Engineers, Part N: Journal of Nanomaterials, Nanoengineering and Nanosystems*, 236(2). doi: 10.1177/09544089211044245

[13] Anitha, L., & Gireesha, B. J. (2023). Convective flow of Jeffrey nanofluid along an upright microchannel with Hall current and Buongiorno model: an irreversibility analysis. *Applied Mathematics and Mechanics*, 44, 16131628. doi: 10.1007/s10483-023-3029-6

[14] Hayat, T., Habibullah, A., Ahmad, B., & Alhodaly, M. S. (2021). Heat transfer analysis in convective flow of Jeffrey nanofluid by vertical stretchable cylinder. *International Communications in Heat and Mass Transfer*, 120, 104965. doi: 10.1016/ j.icheatmasstransfer.2020.104965

[15] Ur Rasheed, H., AL-Zubaidi, A., Islam, S., Saleem, S, Khan, Z., & Khan, W. (2021). Effects of Joule heating and viscous dissipation on magnetohydrodynamic boundary layer flow of Jeffrey nanofluid over a vertically stretching cylinder. *Coatings*, 11(21), 353. doi: 10.3390/coatings11030353

[16] Ullah Khan, S., Ali Shehzadi, S., Munir Abbasi, F., & Hussain Arshad, S. (2021). Thermo diffusion aspects in Jeffrey nanofluid over periodically moving surface with time dependent thermal conductivity. *Thermoscience*, 25(1), 197–207. doi: 10.2298/TSCI190428312U

[17] Dadhich, Y., Jain, R., & Kaladgi, A.R. (2021). Thermally radiated Jeffery fluid flow with nanoparticles over a surface of varying thickness in the influence of heat source. *Case Studies in Thermal Engineering*, 28, 101549. doi: 10.1016/j.csite.2021.101549

[18] Hayat, T., Muhammad, T., Al-Mezal, S., & Liao, S. J. (2016). Darcy-Forchheimer flow with variable thermal conductivity and Cattaneo-Christov heat flux. *International Journal of Numerical Methods for Heat & Fluid Flow*, 26, 2355–2369. doi: 10.1108/HFF-08-2015-0333

[19] Alshomrani, A. S., & Ullah, M. Z. (2019). Effects of homogeneous-heterogeneous reactions and convective condition in Darcy-Forchheimer flow of carbon nanotubes. *Journal of Heat Transfer*, 141(1), 012405. doi: 10.1115/1.4041553

[20] Muhammad, T., Alsaedi, A., Shehzad, S.A., & Hayat, T. (2017). A revised model for Darcy Forchheimer flow of Maxwell nanofluid subject to convective boundary condition. *Chinese Journal of Physics*, 55(3), 963–976. doi: 10.1016/j.cjph.2017.03.006

[21] Mandal, P. K., & Seth, G. S. (2018). Hydromagnetic rotating flow of Casson fluid in Darcy-Forchheimer porous medium. *MATEC Web of Conferences*, 192, 02059. doi: 10.1051/matecconf/201819202059

[22] Bilal Ashraf, M., Hayat, T., Alsaedi, A., & Shehzad, S. A. (2015). Convective heat and mass transfer in MHD mixed convection flow of Jeffrey nanofluid over a radially stretching surface with thermal radiation. *Journal of Central South University*, 22, 1114-1123. doi: 10.1007/s11771-015-2623-6

[23] Hayat, T., Waqas, M., Ijaz Khan, M., & Alsaedi, A. (2017). Impacts of constructive and destructive chemical reactions in magnetohydrodynamic (MHD) flow of Jeffrey liquid due to non-linear radially stretched surface. *Journal of Molecular Liquids*, 225, 302–310. doi: 10.1016/j.molliq.2016.11.023

[24] Ali K., Akbar, M.Z, Farooq Iqbal, M., & Ashraf, M. (2014). Numerical simulation of heat and mass transfer in unsteady nanofluid between two orthogonally moving porous coaxial disks. *AIP Advances*, 4, 107113. doi: 10.1063/1.4897947

[25] Lund, L.A., Omar, Z., Khan, I., Raza, J., Bakouri, M., & Tlili, I. (2019). Stability analysis of Darcy-Forchheimer flow of Casson type Nanofluid over an exponential sheet: Investigation of critical points. *Symmetry*, 11(3), 412. doi: 10.3390/sym11030412

[26] Mabood, F. (2016). Numerical study of unsteady Jeffrey fluid flow with magnetic field effect and variable fluid. *Journal of Thermophysics and Heat Transfer*, 8, 041003. doi: 10.1115/1.4033013

[27] Khani, F., Farmany, A., Ahmadzadeh Raji, M., Aziz, A. & Samadi, F. (2009). Analytic solution for heat transfer of a third grade viscoelastic fluid in non-Darcy porous media with thermophysical effects. *Communications in Nonlinear Science and Numerical Simulation*, 14, 3867-3878. doi: 10.1016/j.cnsns.2009.01.031

[28] Hayat, T., Hussain, Z., Ahmad, B., & Alsaedi, A. (2017). Base fluids with CNTs as nanoparticles through non-Darcy porous medium in convectively heated flow: A comparative study. *Advanced Powder Technology*, 28, 855–865. doi: 10.1016/j.apt.2017.04.003

[29] Siddiq, M. K., Ashraf, M., & Mushtaq, T. (2021). MHD thermally radiative flow of Carreau fluid subjected to the stretching sheet by considering non-Darcy Forchheimer law. *Pramana - Journal of Physics*, 9, 164. doi: 10.1007/s12043-021-02192-z

[30] Madhu, M., & Prabhakar, B. (2021). Darcy-Forchheimer Flow of MHD Powell-Eyring nanoliquid over a nonlinear radially stretching disk with the impact of activation energy. *Discontinuity, Nonlinearity, and Complexity*, 10(14), 743–753. doi: 10.5890/DNC.2021.12.013

[31] Madkhali, H.A., Nawaz, M., Saif, R.S., Afzaal, M.F., Alharbi, S.O., & Kbiri Alaoui, M. (2021). Comparative analysis on the roles of different nanoparticles on mixed convection heat transfer in Newtonian fluid in Darcy-Forchheimer porous space subjected to convectively heated boundary. *International Communications in Heat and Mass Transfer*, 128, 105580. doi: 10.1016/ j.icheatmasstransfer.2021.105580

[32] Machireddy, G.R., Praveena, M.M., Rudraswamy N.G., & Kumar, G.K. (2021). Impact of Cattaneo-Christov heat flux on hydromagnetic flow of non-Newtonian fluids filled with Darcy-Forchheimer porous medium. *Waves in Random and Complex Media*, 1957178. doi: 10.1080/17455030.2021.1957178

[33] Ramesh, G.K., Madhukesh, J.K., Shah, N.A., & Yook, S.-J. (2023). Flow of hybrid CNTs past a rotating sphere subjected to thermal radiation and thermophoretic particle deposition. *Alexandria Engineering Journal*, 64, 969–979. doi: 10.1016/j.aej.2022.09.026

[34] Eswaramoorthi S., Loganathan, K., Faisal, M., Thongchai Botmart, T., & Shah, N.A. (2023). Analytical and numerical investigation of Darcy-Forchheimer flow of nonlinear-radiative non-

Newtonian fluid over a Riga plate with entropy optimization. *Ain Shams Engineering Journal*, 14, 101887. doi: 10.1016/j.asej. 2022.101887

[35] Asghar A., Teh, Y.Y., & Zaimi, K. (2022). Two-Dimensional Mixed Convection and Radiative Al2O3-Cu/H2O Hybrid Nanofluid Flow over Vertical Exponentially Shrinking Sheet with Partial Slip Conditions. *CFD Letters*, 14(13), 22–28. doi: 10.37934/cfdl.14.3.2238

[36] Asghar, A., Lund, L.A., Shah, Z., Vrinceanu, N., Deebani, W., & Shutaywi, M.. (2022). Effect of Thermal Radiation on Three-Dimensional Magnetized Rotating Flow of a Hybrid Nanofluid. *Journal of Nanomaterials*, 12(9), 1566. doi: 10.3390/ nano12091566

[37] Sajjad, M., Mujtaba, A., Asghar A., & Teh Y. Y. (2022). Dual Solutions of Magnetohydrodynamics Al2O3+Cu Hybrid Nanofluid Over a Vertical Exponentially Shrinking Sheet by Presences of Joule Heating and Thermal Slip Condition. *CFD Letters*, 14(8), 100−115. doi: 10.37934/cfdl.14.8.100115

[38] Teh Y.Y., & Asghar, A. (2021). Three Dimensional MHD Hybrid Nanofluid Flow with Rotating Stretching/Shrinking Sheet and Joule Heating. *CFD Letters*, 13(8), 1–19. doi: 10.37934/cfdl. 13.8.119

[39] Asghar, A., Teh, Y.Y., Zaimi, K.. (2022). Two-Dimensional Magnetized Mixed Convection Hybrid Nanofluid Over a Vertical Exponentially Shrinking Sheet by Thermal Radiation, Joule Heating, Velocity and Thermal Slip Conditions. *Journal of Advanced Research in Fluid Mechanics and Thermal Sciences*, 95(2), 159–179. doi: 10.37934/arfmts.95.2.159179

[40] Asghar A., Chandio A.F., Shah Z., Vrinceanu N., Deebani W., Shutaywi M., et al. (2023). Magnetized mixed convection hybrid nanofluid with effect of heat generation/absorption and velocity slip condition. *Heliyon*, 9(2), 13189. doi: 10.1016/j.heliyon. 2023.e13189

[41] Asghar, V., Vrinceanu, N., Teh, Y.Y., Lund, L.A., Shah, Z., & Tirt, V. (2023). Dual solutions of convective rotating flow of three-dimensional hybrid nanofluid across the linearstretching/shrinking sheet. *Alexandria Engineering Journal*, 75, 297–312. doi: 10.1016/j.aej.2023.05.089

[42] Gohar., Khan, T.S., Sene, N., Mouldi, A., & Brahmia, A.(2022). Heat and Mass transfer of the Darcy-Forchheimer Casson Hybrid Nanofluid Flow due to an Extending Curved Surface. *Journal of Nanomaterials*, 3979168. doi: 10.1155/2022/3979168

[43] Sathyanarayana, M., Ramakrishna Goud, T. (2023). Numerical study of MHD Williamson-nano fluid flow past a vertical cone in the presence of suction/injection and convective boundary conditions. *Archives of Thermodynamics*, 44(2), 115–138. doi: 10.24425/ather.2023.146561

[44] Mamatha, S. U., Ramesh Babu, K., Durga Prasad, P., Raju, C.S.K., & Varma, S.V.K. (2020). Mass transfer analysis of two-phase flow in a suspension of microorganisms. *Archives of Thermodynamics*, 41(1), 175-192. doi: 10.24425/ ather.2020.132954

[45] Madhusudhana Rao, B., Gopal, D., Kishan, N., Ahmed, S., & Durga Prasad, P. (2020). Heat and mass transfer mechanism on three-dimensional flow of inclined magneto Carreau nanofluid with chemical reaction. *Archives of Thermodynamics*, 41(2), 223–238. doi: 10.24425/ather.2020.133630

[46] Hayat, T., Shah, F., Hussain, Z., & Alsaedi, A. (2019). Darcy Forchheimer flow of Jeffrey nanofluid with heat generation/absorption and melting heat transfer. *Thermoscience*, 23(6B), 3833−3842. doi: 10.2298/TSCI171222314H

[47] Chandel, S., & Sood, S., (2023). Dynamics of Williamson hybrid nanofluid over an extending surface with non-linear convection and shape factors. *Journal of Nanofluids*, 12 (5), 1335-1350. doi: 10.1166/jon.2023.2022

[48] Nogrehabadi, A., Pourrajab, R., & Ghalembaz, M. (2012). Effect of partial slip boundary condition on the flow and heat transfer of nanofluids past stretching sheet prescribed constant wall temperature. *International Journal of Thermal Sciences*, 54, 253–261. doi: 10.1016/j.ijthermalsci.2011.11.017

[49] Rasool, G., Chamkha, A.J., Muhammad, T., Shafiq, A., & Khan, I. (2020). Darcy-Forchheimer relation in Casson type MHD nanofluid flow over non-linear stretching surface. *Propulsion and Power Research*, 9(2), 159–168. doi: 10.1016/j.jppr.2020.04.003